PCCP

Accepted Manuscript

ROYAL SOCIETY OF CHEMISTRY

www.rsc.org/pccp

Universality in Surface Mixing Rule of Adsorption Strength for Small Adsorbates on Binary Transition Metal Alloys

Jeonghyun Ko[1], Hyunguk Kwon[1], Hyejin Kang[1], Byung-Kook Kim[2], and Jeong Woo Han[1,*]

[1]*Department of Chemical Engineering, University of Seoul, Seoul 130-743, Korea*
[2]*High Temperature Energy Materials Center, Korea Institute of Science and Technology, Seoul 136-791, Korea*

Abstract

Understanding the adsorption phenomena of small adsorbates that involve in a surface reaction on transition metals is important because their adsorption strength can be a descriptor for predicting the catalytic activity. To explore the adsorption energies on a wide range of binary transition metal alloys, however, tremendous computational efforts are required. Using density functional theory (DFT) calculations, here we suggest "*surface mixing rule*" to predict the adsorption energies of H, O, S, CO and OH on bimetallic alloys, based on the linear interpolation of adsorption energies on each pure surface. As an application, the activity of CO oxidation on various bimetallic alloys is predicted from the adsorption energies of CO and O easily obtained by the surface mixing rule. Our results provide a useful tool for rapidly estimating the adsorption energies, and furthermore, the catalytic activities on multi-component metal alloy surfaces.

[*]Correspondence to jwhan@uos.ac.kr

Table of Contents Graphic

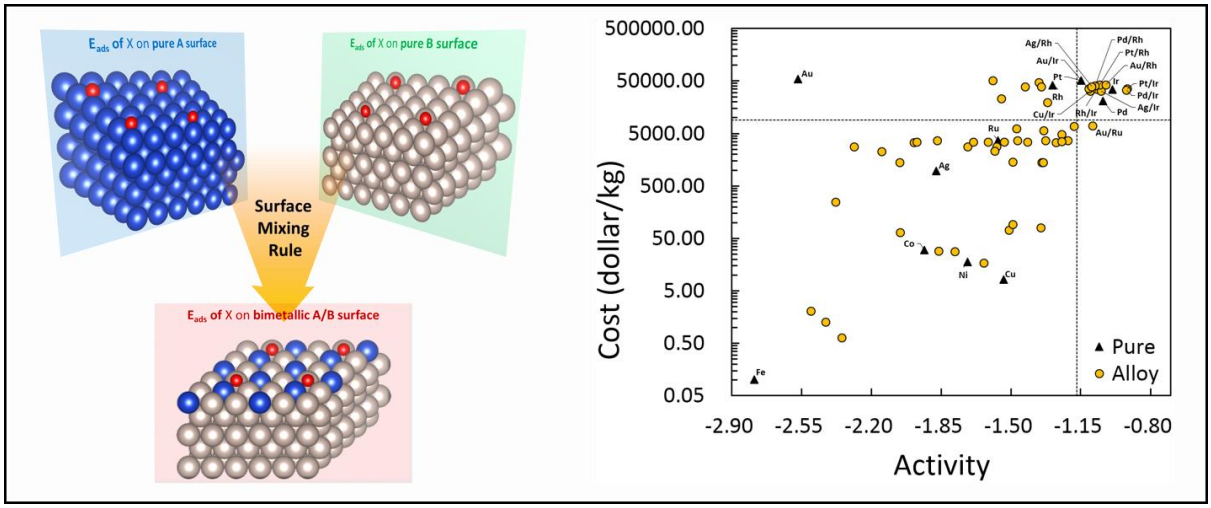

1. Introduction

Transition metals have been widely used as heterogeneous catalysts. Although there have been many attempts to develop transition metal alloy catalysts with better performance and lower price than pure metals, most of them have been relied on experimental trial and error. However, due to recent rapid development of computational capabilities and algorithms, computational approaches such as density functional theory (DFT) have achieved remarkable progress. Thus, it is now possible to rationally design the transition metal alloy catalysts through the fundamental understanding of surface phenomena. The close collaboration between advanced computations and experiments would be the most rational way to study heterogeneous catalysis.

It has been widely known that higher catalytic activity is achieved when the interaction between catalyst and adsorbate should be neither too strong nor too weak.[1] It is therefore important to investigate the adsorption energies of molecules that would participate in the catalytic reaction for estimating the catalytic activity. DFT studies have shown that the adsorption energy is often a key descriptor to describe the surface reaction.[2–6] Logadottir *et al.*[2] found that dissociative adsorption energy of N_2 is an important parameter to predict ammonia synthesis over transition metal catalysts. They estimated that Ru and Fe are placed in the top of the volcano plot under the given operating conditions. Schumacher *et al.*[3] predicted the reactivity of low temperature water-gas shift on transition metals by calculating the adsorption energies of O and CO. Their theoretical prediction was in fairly good agreement with experimental results. Falsig *et al.*[4] proved why nanostructured gold catalyst has higher catalytic activity in CO oxidation reaction using same descriptors as those of Schumacher *et al.*[3] Yoo *et al.*[7] explained the activity and selectivity of formic acid decomposition on transition metal surfaces via the adsorption energies of CO and OH. They theoretically explained that Pd-Au and Pd-Ag alloy catalysts showed good catalytic performance due to the

high H_2 selectivity and suggested a new binary transition metal alloy catalyst, Cu_3Pt, as a good candidate. These examples confirmed that the adsorption energies of reactants and/or intermediates can be a powerful tool to predict the catalytic activity of a surface reaction. It is therefore essential to obtain the adsorption energies on a wide range of transition metal alloy surfaces for rapidly screening the catalytic activity of various reactions on the surfaces.

Solid oxide electrolyzer cell (SOEC) is a promising technology for the production of syngas under high temperature (600 ~ 1000 ℃) via co-electrolysis of H_2O and CO_2. Feeding H_2O and CO_2 gases are simultaneously electrolyzed to generate H_2 / CO gases and oxygen ions on the cathode. The oxygen ions are transported to the anode via solid electrolyte and then oxidized to oxygen gases.[8] The Ni catalyst supported on yttria-stabilized zirconia (YSZ) is conventionally used as the cathode of SOEC due to the higher catalytic activity and less cost than other pure metals.[9] To overcome the current performance of SOEC cathode, it is thus critical to develop new transition metal catalysts which have better activity than Ni with maintaining the price. In this respect, alloying is one of the plausible ways to satisfy these qualifications. By alloying pure transition metals, we may control the strength of adsorption that is a key descriptor of catalytic activity, and simultaneously manufacture the catalysts with a combination of more economic materials. It is therefore important to estimate the adsorption energies on hundreds of transition metal alloy surfaces.

Although DFT calculation is a fast and economic method to calculate the adsorption energies of small adsorbates, tremendous computational efforts are still required to investigate the adsorption energies for a wide range of binary transition metal alloys. It is therefore necessary to develop a simple method for rapidly estimating the adsorption energies on numerous pairs of bimetallic alloys. Greeley *et al.*[10] effectively predicted the adsorption energies of O on alloy surfaces as a function of the *d*-band center shift. Andersson *et al.*[11] also predicted the adsorption energies of O on bimetallic surfaces, using the linear interpolation of adsorption

energies based on the type of the surrounding atoms of adsorption site. The previous studies are, however, founded on several assumptions; the adsorption sites are fixed at 3-fold hollow and all metals exist in the fcc crystal structure. In addition, dispersion force, spin-polarization, surface segregation, various alloying patterns of surface layer, and adsorbates other than O are not considered in the studies.

Here we introduce a simple method to rapidly estimate the adsorption energies of small adsorbates on binary transition metal alloy solely from their adsorption energies on pure metal surfaces. We examine the adsorption behavior of four adsorbates (H, O, CO and OH) that would participate in the co-electrolysis on the metal catalyst of SOEC cathode. These adsorbates also play key roles in describing many catalytic reactions—that are of great industrial importance—on transition metal surfaces such as water-gas shift reaction, CO oxidation, and hydrogen evolution. We also investigate the adsorption of sulfur because the catalyst deactivation caused by sulfur poisoning is one of the most considerable issues. The sulfur contents in the feedstock is strongly adsorbed on transition metal surfaces. Thus, it not only covers the active sites physically but also causes the electronic and geometric changes of the catalysts.

This paper is organized as follows. Firstly, our DFT results of adsorption on pure and bimetallic surfaces are summarized. Then, we introduce *"surface mixing rule*" to quickly estimate the adsorption strength on binary transition metal alloys with discussion of the theoretical origin. Lastly, we show how to apply our surface mixing rule to studying heterogeneous catalysis with an example of CO oxidation.

2. Computational Methods

Periodic density functional theory (DFT) calculations were performed with Vienna Ab Initio Simulation Package (VASP)[12–15] code. Exchange-correlation energies were treated by Perdew-Burke-Ernzerhof (PBE) functional based on generalized gradient approximation

(GGA).[16] All calculations used a plane wave expansion with a cutoff of 400 eV. Total energy calculations were conducted using the residual minimization method for electronic relaxation, accelerated using Methfessel-Paxton Fermi-level smearing[17] with a width of 0.2 eV. Geometries were relaxed using a conjugate gradient algorithm until the forces on all unconstrained atoms were less than 0.03 eV/Å . We considered spin-polarization only when we treat the Ni(111), Co(0001), Fe(110) and their alloys. To avoid the artificial electrostatic filed, dipole corrections were applied in computing all of the energies reported here.[18,19]

For the surface calculations, the DFT-optimized lattice constants listed in Table S1 of supplementary information were used, which are in good agreement with the experimental values[20] (Table S1). (111), (0001) and (110) surfaces are thermodynamically the most stable for face-centered cubic (fcc) (Ni, Cu, Ir, Pt, Pd, Rh, Au and Ag), hexagonal-centered cubic (hcp) (Co and Ru) and body centered cubic (bcc) (Fe) structures, respectively. In case of the surface alloys, the lattice constants and crystal structures of host metals were chosen. The host metal atoms were then substituted with solute metal atoms on the first layer of the host surface up to 1/3, 2/3 and 1 ML. In our models, five-layer slabs and vacuum of 15 Å in the direction of the surface normal were employed for all calculations. The bottom two layers were fixed in their bulk positions while the other top 3 layers were fully relaxed. The (3 × 3) surface unit cells (corresponding to 1/9 ML) and Monkhorst-Pack[21] grid of 3 × 3 × 1 *k*-points were used. For the calculations of gas-phase, the geometries of gas phase molecules were optimized by performing calculations in the large periodically repeated cubic boxes (approximately 20 Å on a side).

In order to take into account for dispersion force, we used semi-empirical DFT-D2 method proposed by Grimme.[22] The dispersion coefficient C_6 for Au(111) and Ir(111) used a value of 40.62 J nm^6/mol and for Pt(111) used a value of 20 J nm^6/mol. The vdW radius R_0 for Au(111) and Ir(111) used a value of 1.772 Å and for Pt(111) used a value of 1.9 Å.[24–28] The

parameters of other metals are referred to original paper of Grimme.[22] We also set the global scaling factor s_6 is 0.75 which was suggested by Grimme for PBE and cutoff radius is 30.0 Å. The dispersion correction is not necessarily required for chemisorbed systems as in this study. However, we employed the correction to consistently apply the results here to our ongoing research [23] for SOEC cathode catalyst which includes CO_2 adsorption and its dissociation on various metal surfaces as mentioned earlier. In addition, our test calculations showed small constant shift in the adsorption energy for each adsorbate, confirming that the dispersion correction would not change our main results in this paper.

The zero-point energy (ZPE) corrections are included in our calculations. To assess the role of zero point energies, normal modes and vibrational frequencies were calculated within the harmonic approximation using finite difference displacements of 0.05 Å. From our test calculations for atomic H adsorption on several metal surfaces, ZPE did not significantly affect the adsorption energy when surface metal atoms were not included in the calculations. Therefore, only adsorbate atoms were included in these calculations but the metal atoms were fixed in their equilibrium position. Once the normal mode frequencies, ν_i, were computed, the total zero-point energy is defined by $\sum_i h\nu_i /2$, where the sum is over all normal modes with real vibrational frequencies.

3. Result

3.1 Adsorption on pure metal and binary metal alloy surfaces

We investigate the adsorption of small adsorbates (H, O, S, CO and OH) on 11 transition metal surfaces such as Ni(111), Fe(110), Cu(111), Co(0001), Ir(111), Ru(0001), Pt(111), Pd(111), Rh(111), Au(111), Ag(111) and their metal alloys. Here we briefly describe the adsorption of small adsorbates on pure metal and binary metal alloy surfaces. A detailed information of adsorption energetics and configurations is described in supplementary

information.

Adsorption on pure metal surfaces For hcp(0001) and fcc(111), there are four adsorption sites; top, 2-fold bridge, hcp hollow and fcc hollow (Fig. S1). For bcc(110), there also exist four adsorption sites; top, short bridge, 3-fold hollow and long bridge (Fig. S1). We investigated all of these adsorption sites in our DFT calculations. The site preferences and adsorption energies on pure metal surfaces are summarized in the Table S2. The high coordination site such as 3-fold hollow site is mostly preferred upon both atomic and molecular adsorption on the pure metal surfaces. For a few bimetallic alloys that have non-hollow site as the most stable site of molecular adsorption, OH often tends to tilt from the plane of the surface while CO remains the vertical adsorption geometry on the surface (Fig. S2).

Adsorption on binary metal alloy surfaces For bimetallic alloy surfaces, if the solute atom tends to remain in the bulk interior rather than on the surface, the effect of alloying would be significantly diminished due to the reduction of active sites.[29,30] We therefore ruled out the binary pairs in which the dopants are not energetically preferred to segregate towards the host surface. From Ruban *et al.*'s database,[31] we select 53 binary metal alloys with preferred surface segregation of solute atoms among the 110 bimetallic alloys that consist of 11 pure metals.

Meanwhile, when we consider bimetallic alloy surfaces, there could be several surface patterns of alloy ordering. Here, we chose the solute coverage of 1/3 ML as a representative of surface alloy composition.[32] 2 patterns (P1 and P2) for fcc and hcp structures and 3 patterns (P3, P4 and P5) for bcc structure were considered (Fig. 1(a)~(e)). We obtained the most stable surface patterns of each alloy from our DFT calculations (Table S3).

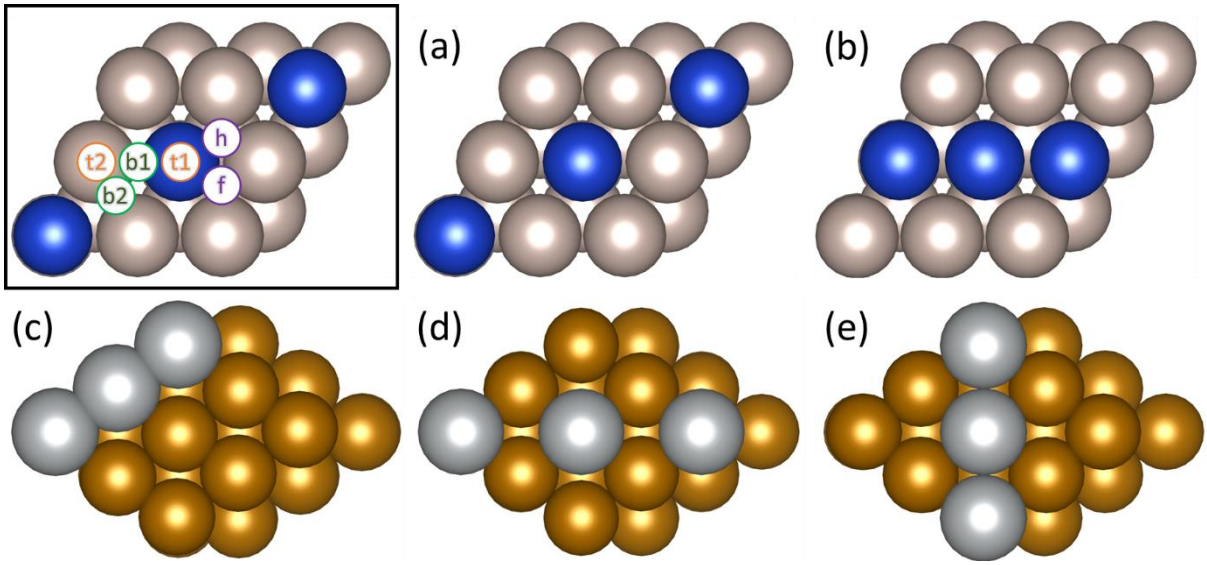

Figure 1: Top view of surface alloy patterns. (a) P1 and (b) P2 pattern of Cu/Ru(0001). (c) P3, (d) P4 and (e) P5 pattern of Ag/Fe(110). The inset box indicates top view of the adsorption sites on Cu/Ru(0001) which has P1 pattern (t1 : top 1, t2 : top 2, b1 : 2-fold bridge 1, b2 : 2-fold bridge 2, h : hcp hollow, f : fcc hollow). Cu, Ru, Ag and Fe atoms are denoted by blue, light gray, gray and dark gold balls, respectively.

Most of adsorption sites on the alloy surfaces are similar to those on the pure metal surfaces, but often slightly different due to the effect of solute atoms. For instance, when the adsorption is occurred on Cu/Ru(0001) with P1 pattern, there are 6 different adsorption sites, depending on the surface pattern of alloying and the surrounding atoms (inset box in Fig. 1). In case of the adsorption at the top site, the adsorbate can be adsorbed right above Cu or Ru atoms (t1 or t2 sites). For the adsorption at 2-fold bridge, there are two types of adsorption; the adsorption between Cu and Ru atoms (b1) and between two Ru atoms (b2). For the adsorption at hcp (or fcc) hollow, there is only one site in which an adsorbate is surrounded by one Cu and two Ru atoms (h or f). The results of adsorption on the bimetallic surfaces are summarized in the Table S4. For atomic adsorption, the high coordination sites such as hollow site are usually favored. For molecular adsorption, however, the low coordination site such as top site can also be stable on various surfaces. Similarly to the pure surfaces, OH is tilted in most cases when it stably adsorbs on the non-hollow sites of alloys surfaces, but CO sticks to vertically bind onto the

bimetallic alloy surfaces.

3.2 Surface mixing rule of adsorption strength on binary transition metal alloys

We examined the adsorption energies and site preferences of various adsorbates (H, O, S, CO and OH) on both pure and alloy surfaces through the DFT calculations. Since the adsorption energies vary with the components of alloy metals and their compositions, huge computational costs would be required to calculate all of them for hundreds of bimetallic alloy surfaces. Here we suggest a simple method to predict the adsorption energies on binary alloy surfaces from the adsorption energies on their surface of each component. We denote it as "*surface mixing rule*" in which the adsorption energy depends on the alloy's component and coverage of solute metals. The binary alloy surfaces are significantly influenced by the component and coverage of upper most layer of the surfaces. We estimate the adsorption energy on bimetallic surfaces using the weighted average of that on each pure component. For example, we found that atomic O adsorbs at fcc hollow site on Rh/Ir(111) surface (section S3 of the supplementary information). The top layer of Rh/Ir(111) in the unit cell consists of three Rh atoms (solute) and six Ir atoms (host). In this case, we can predict the adsrotpion energy of atomic O on Rh/Ir(111) by using

$$\left[E_{ads}(O)\right]_{Rh/Ir(111)} = \frac{1}{3}\left[E_{ads}(O)\right]_{Rh(111)} + \frac{2}{3}\left[E_{ads}(O)\right]_{Ir(111)},$$

where the square brackets indicate the adsorption energy of atomic O on the subscripted metal surfaces. The adsorption energy of atomic O on Rh/Ir(111) esimated from the surface mixing rule is -2.04 eV, which is precisely same as our DFT-calculated adsorption energy. Fig. 2 shows the comparison of the adsorption energies predicted by the surface mixing rule with DFT-calculated ones, which is in fairly good agreement. By using the surface mixing rule, we can reasonably assess the adsorption energies on binary alloy surfaces (The root mean square errors

(RMSEs) of H, O, S, CO and OH are 0.14, 0.30, 0.33, 0.28 and 0.24 eV, respectively).

In addition, in order to prove that the surface mixing rule is valid in the wide range of solute coverages other than 1/3 ML, we performed further calculations to obtain the adsorption energies of H, O, S, CO and OH on both Rh/Ir(111) and Ir/Ru(0001) with solute coverages of 2/3 and 1 ML, respectively. In case of Rh/Ir(111), we denote Ir as host and Rh as solute because all slab layers consist of Ir except the uppermost layer (Fig. S4). For Ir/Ru(0001), we denote Ru as host and Ir as solute in the same manner. For 2/3 ML of solute coverage, the uppermost layer of bimetallic alloy in the unit cell consists of six solute atoms and three host atoms while 1 ML of solute coverage indicates that the top layer is made up of nine solute atoms. As shown in Fig. 2(b), the surface mixing rule works quite well, even for the extreme condition like a 1 ML when the absolute ratio of nearest-neighbor distance ($d_{solute\text{-}host} = d_{solute\text{-}solute} / d_{host\text{-}host}$, see Fig. S5) is within 1% (0.90 % for Rh/Ir(111) and 0.42 % for Ir/Ru(0001)) (Sec. S4 of supplementary information). We therefore conclude that our surface mixing rule is "*universally*" valid in not only different kinds of adsorbates but also different range of solute coverages within 1% $d_{solute\text{-}host}$.

We recognize that especially for 1 ML solute coverage, however, the adsorption energy is largely influenced by the effect of strain between the different elements as in the previous reports.[33–35] If $d_{solute\text{-}host}$ is much larger than 1%, the accuarcy of the surface mixing rule can be reduced. The surface mixing rule is therefore not appropriate to apply to the systems significantly affected by the strain. The monolayer bimetallic alloys have been often used to understand the properties of the core-shell type alloy models.[36–38] The core-shell type alloy is thus one example that our surface mixing rule may not be applicable to.

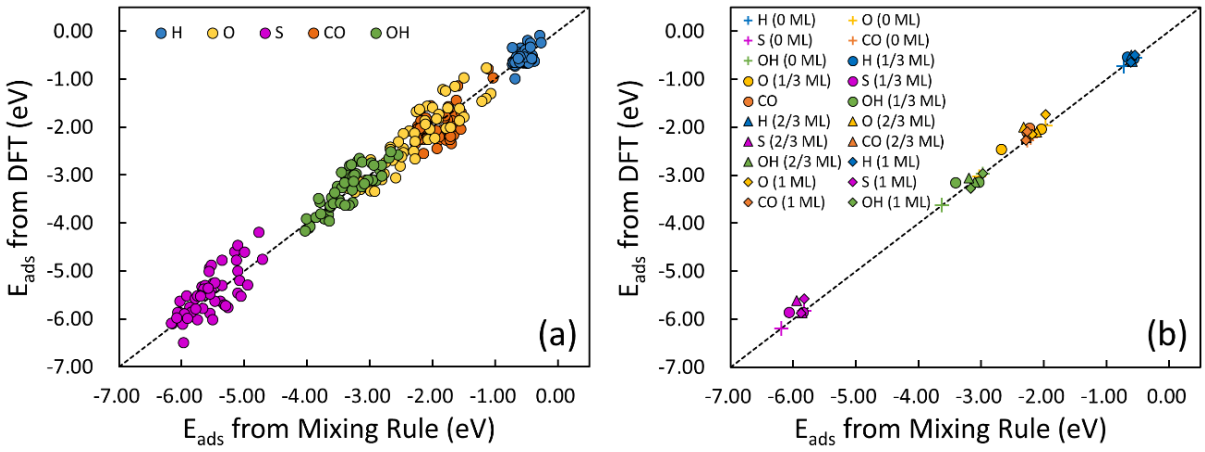

Figure 2: (a) Comparison of the adsorption energies calculated by DFT with the predicted adsorption energies from surface mixing rule. The black dashed line is the identity line. (b) The adsorption energies of H, O, S, CO and OH on Rh/Ir(111) and Ir/Ru(0001) with various host coverages (0, 1/3, 2/3 and 1 ML). The *x*-axis is the values from the surface mixing rule while the *y*-axis is the values obtained by our DFT calculations. The black dashed line is the identity line.

Nørskov *et al.*[39–41] and Pallassana *et al.*[42] described the trend of adsorption energies on binary alloy surfaces in terms of surface *d*-band center (ε_d). Briefly, if ε_d (relative to the Fermi level) is placed in the higher energy state, the adsorbate more strongly adsorbs on the surface. This result indicates that the adsorption energy is closely relevant to the electronic property (represented by ε_d) of transition metal surface.

As shown in Fig. 3, we demonstrate that the weighted average 1st layer ε_d of each pure metal can successfully predict the 1st layer ε_d of binary transition metal alloys. The deviation from the identity line (RMSE) is 0.19 eV. Due to the magnetic effects, the deviations of alloys that contain Ni, Co and Fe (ferromagnetism) are slightly larger. A similar observation was reported in Greeley *et al.*'s previous study.[10] They showed that due to the magnetic effects, the DFT-calculated adsorption energies of O on Fe-contained alloys were more decreased compared to those of their prediction based on ε_d shift.

The electronic property of the topmost layer of an alloy surface is largely influenced by its composition of constituent elements, and can also be predicted by surface mixing rule. It is

thus thought to be an origin of theoretical framework for the surface mixing rule of adsorption energy.

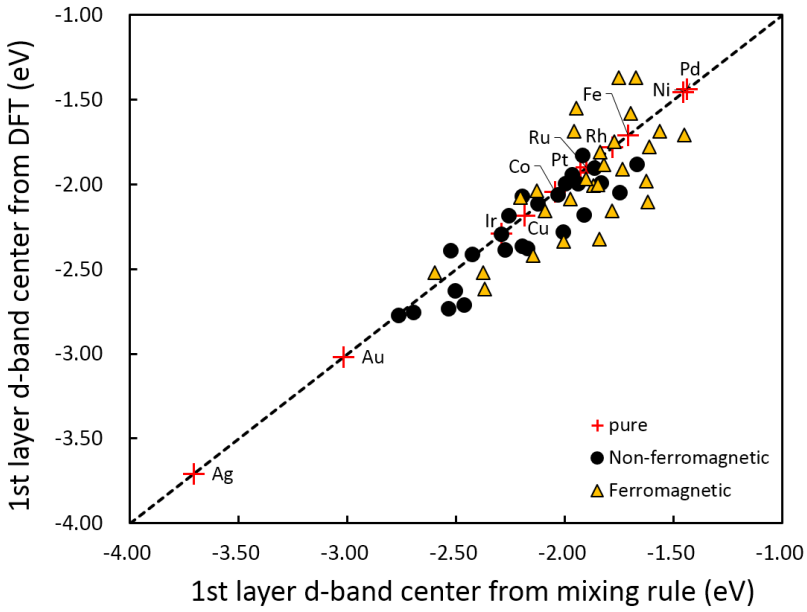

Figure 3: The surface mixing rule for *d*-band center of 1st layer in metal alloy surfaces. The *d*-band centers of 1st layer for non-ferromagnetic and ferromagnetic alloys are denoted by circle and triangle, respectively. The *d*-band centers of 1st layer for pure metals are denoted by red-cross symbol.

3.3 Origin of small deviation on surface mixing rule

When the alloy surface has P2 pattern with hcp or fcc structure, slight deviation between the DFT-calculated adsorption energies and the adsorption energies predicted from surface mixing rule is observed. This may be attributed to the atomic configuration of adsorption sites on bimetallic alloy surfaces. Depending on the surrounding atoms of adsorption site, the P2 pattern has three types of hollow sites of adsorption; solute-solute-host, solute-host-host, and host-host-host (Fig. 4). As we mentioned earlier, we chose the 53 binary metal alloys which prefer to the surface segregation of solute atoms. Interestingly, for the majority of pairs of bimetallic alloys we chose, the adsorption strength of host metals is generally much larger than that on solute metals. Thus, most adsorbates energetically prefer to bind onto the host-host-host hollow site (Fig. 4(b)). In this case, its adsorption energy is dominantly influenced by the host metal.

Since the local electronic structure of this adsorption site is closer to the pure host metal surface than the overall uppermost surface of the alloy, surface mixing rule may provide the slight deviated predictions. Here we define the hollow site composed of solute-host-host as "ideal site". It has same solute-host ratio (=1/3) as the overall alloy surface in the uppermost layer. The ideal site is thus expected to exhibit similar electronic structure to the entire alloy surface of the uppermost layer. Fig. 5 shows the comparison of the DFT-calculated adsorption energies with the adsorption energies estimated from the surface mixing rule on hcp and fcc P2 pattern surface structures. The adsorption energies at the ideal sites are quite well-fit with an identity line compared to the most stable sites. The ideal sites are not always same as the most stable sites because the adsorbates tend to bind on the site adjacent to the energetically attractive metal atoms which is the host-host-host hollow site in P2 pattern.

Except for the reason mentioned above, there still remain the source of the slight deviations of the surface mixing rule on some alloy surfaces (Pt/Ni, Au/Ni, Pd/Cu, Au/Cu, Pt/Co, Au/Co and Co/Ru), which is dominantly caused by the strain effect.[33] For these bimetallic alloys, the $d_{solute\text{-}host}$ are pretty large (Pt/Ni: 12.75 %, Au/Ni: 18.41 %, Pd/Cu: 8.79 %, Au/Cu: 14.84 %, Pt/Co: 13.02 %, Au/Co: 18.70 % and Co/Ru: 8.79 %).

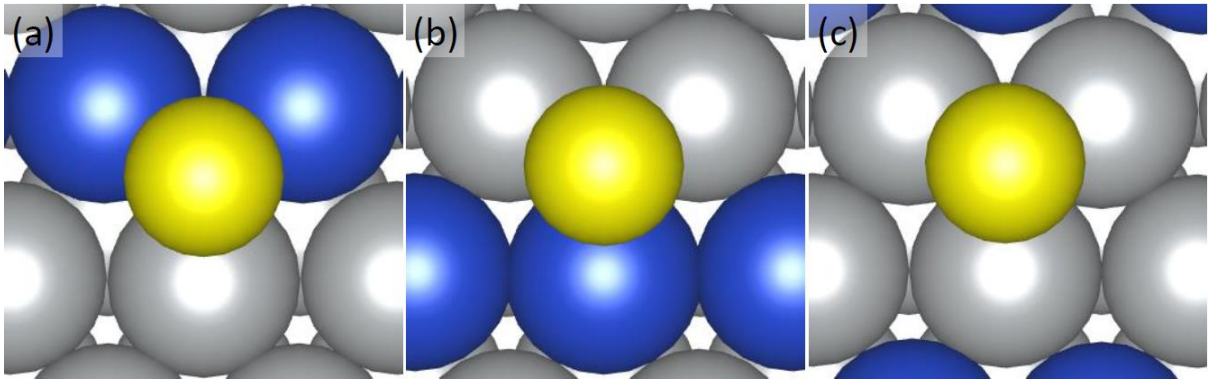

Figure 4: Configuration of the neighboring atoms when adsorption occurs at hollow site. (a) solute-solute-host, (b) solute-host-host (ideal site) and (c) host-host-host. Solute, host and adsorbate atoms are denoted by blue, gray and yellow balls, respectively.

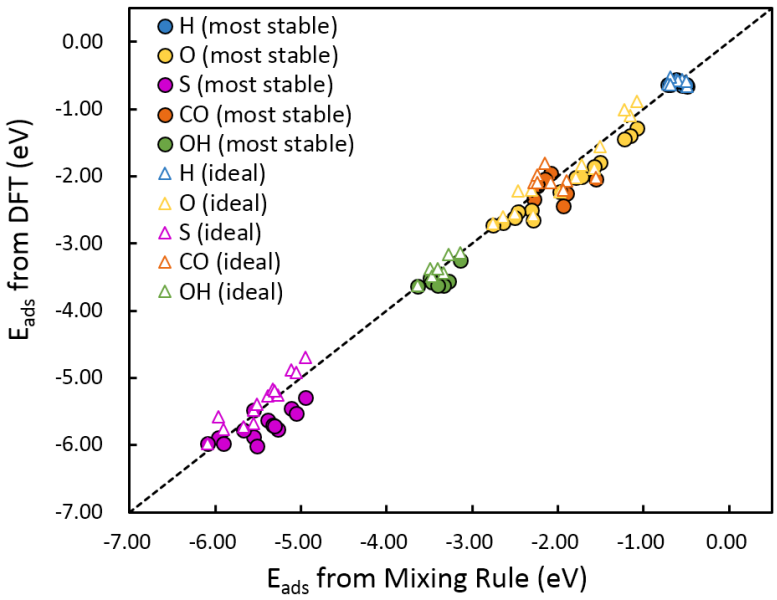

Figure 5: Comparison of the DFT-calculated adsorption energies at the most stable and the ideal site with the predicted adsorption energies from the surface mixing rule on hcp and fcc P2 pattern surface structure. Adsorption energies at the most stable and the ideal site are denoted by filled circle and unfilled triangle, respectively.

3.4 Application of surface mixing rule to predict the catalytic activities on binary transition metal alloys

In this section, we introduce how the surface mixing rule can be applied to predict the catalytic activity of CO oxidation on binary transition metal alloys. As mentioned earlier, Falsig *et al.*[4] assessed the catalytic activity of CO oxidation on pure metal surfaces through the microkinetic model based on the adsorption energies of intermediates and the activation energy barriers of each elementary step.[4,43,44] They proved that adsorption energies of O and CO are the descriptors of the activity of CO oxidation. To explore the candidates of bimetallic alloy catalysts with higher activity, we obtain the adsorption energies of O and CO on binary transition metal alloy surfaces via the surface mixing rule (Fig. 6(a)). We select the alloys with solute coverage of 1/3 ML as before. Note that their values of adsorption energy are a bit different from our data due to the usage of different functional and method of DFT modeling. They used a RPBE functional and four layer slab model with DACAPO code while we

employed a PBE-D2 functional and five layer slab model with VASP code (details in Sec. 2). In order to include the adsorption energies on Fe(110), Co(0001), and Ir(111) which they did not consider, therefore, we made correction by adding the average of differences between Falsig *et al.*'s and our adsorption energies on pure metal surfaces to our adsorption energies (Table S7). The corrected adsorption energies are summarized in Table S7. For example, in the case of binary metal alloys that contained Fe, Co and Ir, $[E_{ads}(O)]_{Rh(111)}$ is taken from Falsig *et al.*'s[4] and the corrected adsorption energy is used as $[E_{ads}(O)]_{Ir(111)}$ to predict the adsorption energy of O on Rh/Ir(111) via the surface mixing rule. We then estimate the catalytic activity of binary metal alloy surfaces using their microkinetic model based on the predicted adsorption energeis of O and CO (T = 600 K, P_{O2} = 0.33 bar and P_{CO} = 0.67 bar). Fig. 6(a) shows a theoretical volcano plot of Sabatier activity for CO oxidation on pure metals and their alloy surfaces as a function of adsorption energies of O and CO (see also Table S8). As a result, we found that several pairs of bimetallic catalysts (Pt/Ir, Pd/Ir, Au/Rh, Ag/Ir, Pt/Rh, Rh/Ir, Pd/Rh, Au/Ru, Ag/Rh, Cu/Ir and Au/Ir) will promise the higher activity of CO oxidation than Pd and Pt. As described in Sec. 3.1, the stability of bimetallic alloys was taken into account based on surface segregation and surface patterns of alloy ordering in this predicition.

Improving economic efficiency is also one of the important issues for design of alloy catalysts. Thus, we conducted the economic evaluation based on data in ref.[45]. The cost of binary transition metal alloys is calculated from each commodity price of constituent metals. Fig. 6(b) shows the cost and activity for CO oxidation at various pure metals and binary metal alloys (see also Table S8). In the upper right side, there are several binary metal alloy catalysts which have higher activity than Pd (reported to have the highest activity by Falsig *et al.*[4]). Through the surface mixing rule, we found that Pt/Ir, Pd/Ir and Au/Rh have remarkable catalytic activity. Unfortunately, their price is pretty expensive. In the bottom right side, however, there is a binary metal alloy catalyst, Au/Ru, which have not only fairly good catalytic

activity but also less cost than the other alloy catalysts in the upper right side. Au/Ru has higher activity with lower cost than Pt, so it can be a good candidate as the catalyst of CO oxidation. Bimetallic Au/Ru catalyst has also been known as its good activity for water-gas shift reaction.[46] As a result, our approach (surface mixing rule, microkinetic model and economic evaluation) provides very helpful insight for screening the binary metal alloy catalysts for CO oxidation as well as possibly other heterogeneous catalysis.

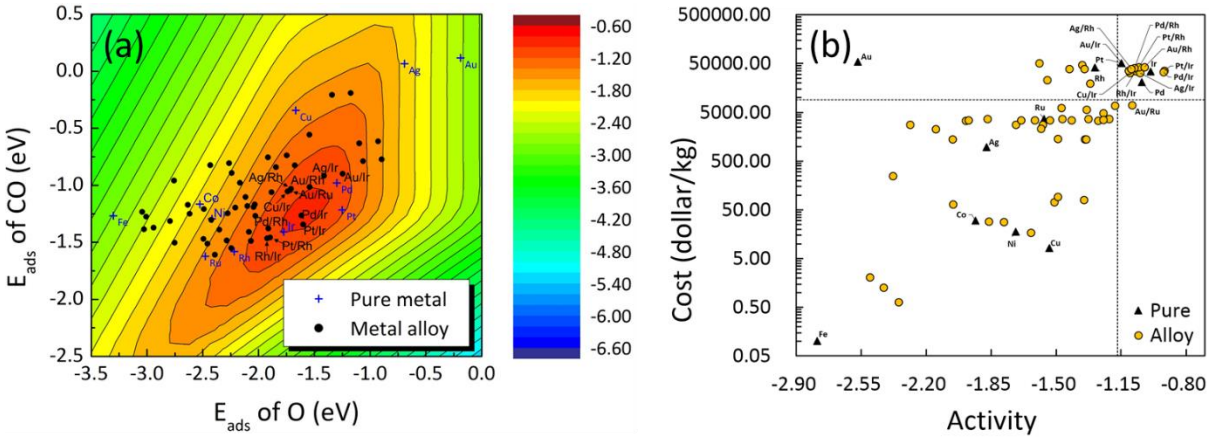

Figure 6: (a) Activity of CO oxidation described as the adsorption energies of O and CO at T = 600 K, P_{O2} = 0.33 bar and P_{CO} = 0.67 bar (Activity = $kT\ln(r_s/\nu)$ and $\nu = kT/h$, where k is the Boltzmann constant, T is the absolute temperature, r_s is the Sabatier rate, and h is the Planck constant, detail in ref. [4]). The pure metals and alloys are denoted by blue cross and black circle symbols, respectively. The adsorption energies on pure metal surfaces are calculated from Falsig *et al.*[4] and the adsorption energies on binary metal alloy surfaces are estimated by surface mixing rule. (b) Graph for cost vs. activity for CO oxidation at various pure metals and binary metal alloys. The pure metals and alloys are denoted by black triangle and yellow circle symbols, respectively. This figure is based on research by Falsig *et al.*[4]

4. Conclusion

In heterogeneous catalysis, the adsorption energy of small adsorbates that involve in a surface reaction on transition metals is often a key parameter to estimate the catalytic activity. Due to the tremendous computational efforts, however, it is very challenging to calculate the adsorption energies of each adsorbate on numerous transition metal alloys via DFT calculations. In this study, we suggested a method, "*surface mixing rule*", to simply predict the adsorption

energies of small adsorbates (H, O, S, CO and OH) on a wide of binary metal alloy surfaces, solely from their adsorption energies on the pure metal surfaces. For more rigous investigation of adsorption phenomena than previous studies,[10,11] we have considered surface segregation and surface ordered patterns of bianry metal alloys, site preference of the adsorption, spin-polarization, dispersion force, and zero-point energy. We also confirmed that the surface mixing rule is valid in the different range of solute coverages within 1% $d_{solute\text{-}host}$.

We found that it is also possible to predict the ε_d of binary transition metal alloys using weighted average ε_d of each pure metal, which may be an origin of the surface mixing rule. There can exist small deviations of the surface mixing rule caused by the ensemble of atoms surrounding the adsorbate and the effect of strain generated by lattice mismatch between solute and host metals. These are points to be considered in predicting the adsorption characteristics of bimetallic alloys through the surface mixing rule.

Lastly, based on the existing study for CO oxidation,[4] we applied the surface mixing rule to the prediction of the adsorption energies of O and CO, which are decriptors of the reaction, on various binary transition metal alloy catalysts. Combining the predicted catalytic activity with the economic evaluation, we suggested the bimetallic Au/Ru catalyst as a good catalyst candidate for CO oxidation. As our future research, we will develop microkinetic models to estimate the catalytic activity of co-electrolysis in SOEC cathode based on simple descriptors for tayloring the catalysts of enhanced performace compared to the conventional Ni. Our results will provide a useful insight for screening heterogeneous catalysts with high performance by rapidly estimating the adsorption energies on multi-component metal alloy surfaces.

Acknowledgement

The authors acknowledge the financial support from the KIST Institutional Program (2E24021-13-031) and Basic Science Research Program through the National Research Foundation of

Korea (NRF) funded by the Ministry of Science, ICT & Future Planning (2014R1A1A1005303), and the supercomputing resource including technical support from Supercomputing Center/Korea Institute of Science and Technology Information (KSC-2013-C1-019).

References

[1] P. Sabatier, Berichte Der Dtsch. Chem. Gesellschaft. 44 (1911) 1984–2001.

[2] A. Logadottir, T.H. Rod, J.K. Nørskov, B. Hammer, S. Dahl, C.J.H. Jacobsen, J. Catal. 197 (2001) 229–231.

[3] N. Schumacher, A. Boisen, S. Dahl, A.A. Gokhale, S. Kandoi, L.C. Grabow, J.A. Dumesic, M. Mavrikakis, I. Chorkendorff, J. Catal. 229 (2005) 265–275.

[4] H. Falsig, B. Hvolbaek, I.S. Kristensen, T. Jiang, T. Bligaard, C.H. Christensen, J.K. Nørskov, Angew. Chem. Int. Ed. Engl. 47 (2008) 4835–9.

[5] T. Bligaard, J.K. Nørskov, S. Dahl, J. Matthiesen, C.H. Christensen, J. Sehested, J. Catal. 224 (2004) 206–217.

[6] M. Mavrikakis, Nat Mater. 5 (2006) 847–848.

[7] J.S. Yoo, F. Abild-Pedersen, J.K. Nørskov, F. Studt, ACS Catal. 4 (2014) 1226–1233.

[8] H. Minfang, F. Hui, P. Suping, Eng. Sci. 12 (2014) 43–50.

[9] M. Ni, M.K.H. Leung, D.Y.C. Leung, Int. J. Hydrogen Energy. 33 (2008) 2337–2354.

[10] J. Greeley, J.K. Nørskov, Surf. Sci. 592 (2005) 104–111.

[11] M. Andersson, T. Bligaard, A. Kustov, J. Catal. 239 (2006) 501–506.

[12] G. Kresse, J. Furthmüller, Phys. Rev. B. 54 (1996) 11169–11186.

[13] G. Kresse, J. Hafner, Phys. Rev. B. 47 (1993) 558–561.

[14] G. Kresse, J. Hafner, J. Phys. Condens. Matter. 6 (1994) 8245.

[15] D.S. Sholl, J. Steckel, A. Density functional theory: a practical introduction, John Wiley & Sons, Inc., Hoboken, New Jersey, 2009.

[16] J.P. Perdew, K. Burke, M. Ernzerhof, Phys. Rev. Lett. 77 (1996) 3865–3868.

[17] M. Methfessel, A.T. Paxton, Phys. Rev. B. 40 (1989) 3616–3621.

[18] L. Bengtsson, Phys. Rev. B. 59 (1999) 12301–12304.

[19] J. Neugebauer, M. Scheffler, Phys. Rev. B. 46 (1992) 16067–16080.

[20] M.J. Winter, Univ. Sheff. WebElements Ltd, UK. (n.d.)., http://webelements.com/.

[21] H.J. Monkhorst, J.D. Pack, Phys. Rev. B. 13 (1976) 5188–5192.

[22] S. Grimme, J. Comput. Chem. 27 (2006) 1787–1799.

[23] J. Ko, B.-K. Kim, J.W. Han, In preparation (2014).

[24] M. Amft, S. Lebègue, O. Eriksson, N. V Skorodumova, J. Phys. Condens. Matter. 23 (2011) 395001.

[25] S. V Aradhya, M. Frei, M.S. Hybertsen, L. Venkataraman, Nat Mater. 11 (2012) 872–876.

[26] P.V.C. Medeiros, G.K. Gueorguiev, S. Stafström, Phys. Rev. B. 85 (2012) 205423.

[27] L. Meng, R. Wu, L. Zhang, L. Li, S. Du, Y. Wang, H.-J. Gao, J. Phys. Condens. Matter. 24 (2012) 314214.

[28] J. Sławińska, I. Zasada, Phys. Rev. B. 84 (2011) 235445.

[29] J.R. Chelikowsky, Surf. Sci. 139 (1984) L197–L203.

[30] J.W. Han, J.R. Kitchin, D.S. Sholl, J. Chem. Phys. 130 (2009) 124710.

[31] A. V Ruban, H.L. Skriver, J.K. Nørskov, Phys. Rev. B. 59 (1999) 15990–16000.

[32] J. Greeley, J.K. Nørskov, Electrochim. Acta. 52 (2007) 5829–5836.

[33] M. Mavrikakis, B. Hammer, J. Nørskov, Phys. Rev. Lett. 81 (1998) 2819–2822.

[34] D. V Esposito, S.T. Hunt, A.L. Stottlemyer, K.D. Dobson, B.E. McCandless, R.W. Birkmire, J.G. Chen, Angew. Chem. Int. Ed. Engl. 49 (2010) 9859–62.

[35] S. Sakong, C. Mosch, Phys. Chem. Chem. Phys. 9 (2007) 2216–2225.

[36] D.A. Hansgen, D.G. Vlachos, J.G. Chen, Nat. Chem. 2 (2010) 484–489.

[37] M.K. Sabbe, M.-F. Reyniers, K. Reuter, Catal. Sci. Technol. 2 (2012) 2010–2024.

[38] J.G. Chen, C.A. Menning, M.B. Zellner, Surf. Sci. Rep. 63 (2008) 201–254.

[39] B. Hammer, J.K. Nørskov, Surf. Sci. 343 (1995) 211–220.

[40] A. Ruban, B. Hammer, P. Stoltze, H.L. Skriver, J.K. Nørskov, J. Mol. Catal. A Chem. 115 (1997) 421–429.

[41] F. Abild-Pedersen, J. Greeley, J. Nørskov, Catal. Letters. 105 (2005) 9–13.

[42] V. Pallassana, M. Neurock, J. Catal. 191 (2000) 301–317.

[43] S. Dahl, J. Sehested, C.J.H. Jacobsen, E. Törnqvist, I. Chorkendorff, J. Catal. 192 (2000) 391–399.

[44] C. Ovesen, B. Clausen, J. Catal. 180 (1996) 170–180.

[45] Mineral commodity summaries 2013: U.S. Geological Survey, 2013.

[46] A. Venugopal, J. Aluha, D. Mogano, M.S. Scurrell, Appl. Catal. A Gen. 245 (2003) 149–158.